



# A new tool for the rheometric study of oil well cement slurries and other settling suspensions

Voula Vlachou<sup>1</sup>, Jean-Michel Piau\*

*Laboratoire de Rhéologie, Universités de Grenoble (UJF and INPG), CNRS (UMR5520), BP 53, Dom. Universitaire, 38041 Grenoble Cedex 9, France*

Received 22 July 1999; accepted 21 July 2000

## Abstract

An original rheometric geometry has been used in order to solve experimental problems related to the study of suspensions of coarse, heavy particles. This testing device has been used to characterize oil well cement slurries, which are settling suspensions of big industrial interest. The measurements show that the new geometry remedies efficiently for settlement and slip at the walls. Results are compared with those obtained using conventional geometries, and reveal the importance of the errors to which non-adapted instruments can lead. © 2000 Elsevier Science Ltd. All rights reserved.

**Keywords:** Rheology; Oil well cement; Microstructure; Physical properties; Rheometry

## 1. Introduction

Cement slurries are used for sealing oil and gas wells, water wells, waste disposal wells, and geothermal wells, in order to isolate the zones encountered while drilling. The rheological behavior of the cement slurry is a component of outmost importance for the design of the cementing process. Only if slurry rheological properties are well characterized can friction pressure drop and flow regime in the annulus be predicted correctly. However, this characterization is difficult, from the experimental standpoint. Cement slurries are concentrated suspensions of coarse, heavy particles, and rheological measurements suffer from several perturbing effects. These include slip at the walls of the measuring device [1–5], migration of the particles due to centrifugal forces [1,3], shear-induced migration [6–10], or gravity-induced migration (settlement). A review of the literature concerning these perturbing effects is made in Ref. [11], pp. 90–95.

Some specific devices have been developed for the rheometric characterization of cement slurries or other

settling suspensions. They usually attempt to maintain a homogeneous composition of the slurry throughout the gap, and reduce the tendency of the particles to migrate by introducing a secondary flow. Bhatti and Banfill [12] used an “interrupted helical impeller” coaxial rheometer. Angled blades fixed on the inner cylinder (bob) are supposed to provide sufficient mixing action to give negligible sedimentation of the paste. Meeten [13] suggested a “pumped-cup” coaxial rheometer. An external pump provides a circulation of the fluid through the sample cup and around the rotor–stator assembly. This circulation mixes and homogenizes the fluid, and prevents solids built-up in both the annular gap and the cup bottom.

The original idea of locating grid tools in the bulk of samples has been used in Refs. [14–16] for the study of aqueous concentrated suspensions. A modified cone and plate geometry was built, where the cone and the plate were made from a grid with openings big enough for particles to settle through them. The grids were submerged in the sample, avoiding, in this way, measurements in the upper and lower zones of the sample. They found that this tool was efficient against errors due to settlement, especially for relatively liquid suspensions with weak structures.

Measurements in the bulk of the sample have also been suggested by Klein et al. [17]. They used an alternative to the coaxial cylinder geometry to measure the rheological properties of coarse suspensions exhibiting settling proper-

\* Corresponding author. Tel.: +34-4-76-82-51-70; fax: +33-4-76-82-51-64.

E-mail address: jmpiau@ujf-grenoble.fr (J.-M. Piau).

<sup>1</sup> Present address: Borregaard LignoTech, PO Box 162, Sarpsborg, Norway.

ties. They positioned the bob in an elongated cup so that measurement is made within a constant density zone of the settling suspension, away from the upper and lower zones. They cut vertical grooves in the shearing surfaces of the cup and bob to reduce wall slip errors, and used narrow gap sizes to lessen non-Newtonian shear rate effects. The device was used for the rheological characterization of magnetite aqueous suspension.

## 2. The new rheometric tool

### 2.1. Description of the fixture

The new geometry constructed to measure the rheological properties of cement slurries is a modified parallel-plate geometry that can be attached to any commercial rotational rheometer. A schematic diagram of the geometry is shown in Fig. 1. The fundamental unit (unit repeated to construct the whole fixture) of the geometry is shown in Fig. 2. It is similar to a geometry already developed by Maxwell [18] to measure the viscosity of air. The fixture consists of a combination of six parallel-plate configurations (that will be called “components” in the following) placed the one over the other. Each plate carries radial openings of about 2

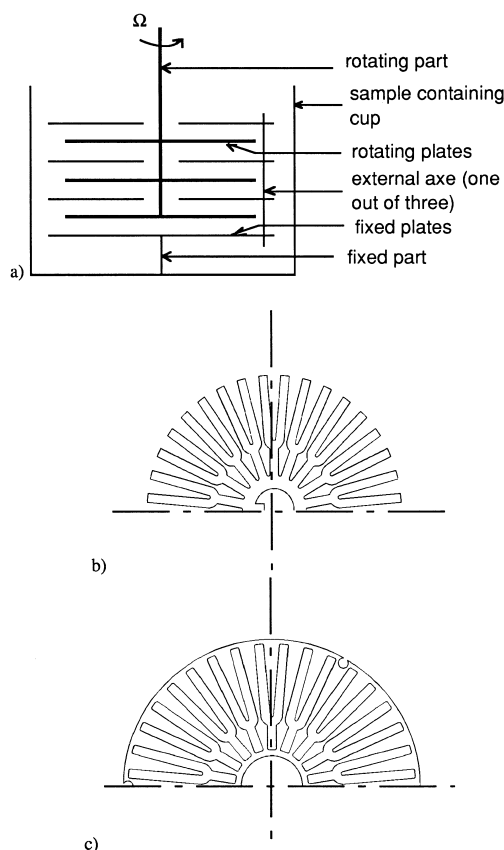
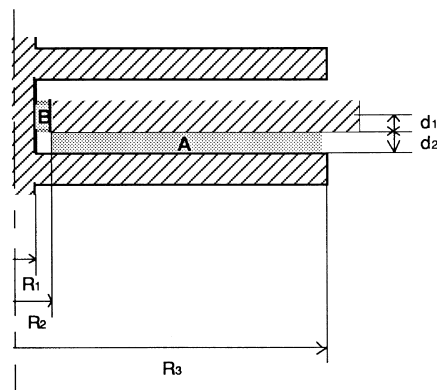


Fig. 1. Schematic drawing of the new fixture: (a) cross-section of the fixture; (b) top view of a rotating plate; (c) top view of a fixed plate.



$d_1 = 1.5 \text{ mm}$   
 $d_2 = 2.0 \text{ mm}$   
 $R_1 = 4.0 \text{ mm}$   
 $R_2 = 7.0 \text{ mm}$   
 $R_3 = 28 \text{ mm}$

Fig. 2. Detailed diagram of three successive plates of the new geometry.

mm. One could say that the rotating plates look like Mexican spurs. These openings allow the particles to freely settle through them and prevent their accumulation on the surface of each plate. They also accomplish a secondary role by providing a roughness to the plates: the openings simulate a grid surface that should prevent or reduce wall slip effects. The measuring system is placed in a cup that contains the sample to be tested. A space of about 1 cm from the bottom and the top of the cup is left free. In this way, the zones of the sample that are rapidly affected by settlement do not participate in the measurement. In fact, the height of the free spaces can be modified by removing the upper and lower pairs of plates (the plates are designed to be removable). This allows adapting the geometry to suspensions with more or less important settling velocities, or to experimental procedures of more or less long duration. Moreover, by changing the number of plates used, the sensitivity limits of the rheometer can be extended, since the measured torque is proportional to a factor corresponding to the number of components used.

The distance between successive plates (gap) was fixed at 2 mm. This value has been chosen in order to comply with the empirical rule, according to which the gap must be at least 20 times the nominal diameter of the biggest particles. With this condition, the hypothesis of continuous medium should be respected, for cement slurries for which the maximum particle diameter is about  $100 \mu\text{m}$  (see particle size distribution in Fig. 4).

The diameter of the plates has been defined in order to keep the ratio  $R_2/R_3$  (see Fig. 2) small. With the dimensions chosen, this ratio is of  $1/4$ . As it can be seen in Appendix A, the radius appears in the third power in the expression of the measured torque. Therefore, the error induced in the torque value because of the absence of the central part of the plates is theoretically less than 1% is shown in Appendix A, with

these dimensions, the results are only marginally affected by the absence of the central part of the plates.

The new geometry has been used with two laboratory rheometers: the Carrimed CS100, a torque-controlled rheometer, and the Carrimed Weissenberg Rheogoniometer, a rotational speed-controlled rheometer. In the CS100 configuration, the sample container and the four larger plates are stationary. The torque is applied to the axis that joins together the three smaller plates. The generated angular velocity is measured on the same axis. In the Weissenberg version, the cup containing the sample is rotating, driving the system of the four larger plates, and the resulting torque on the three smaller plates is measured. In the following, the rotating and non-rotating parts will be called rotor and stator, respectively.

## 2.2. Rheometric calculations

The flow between two plates of our geometry can be decomposed in two parts (see Fig. 2): a flow between two parallel plates in the Region A, and a flow between two coaxial cylinders in the Region B. It can be shown (see Appendix A) that the torque resulting from the flow in Region B is negligible compared to the torque corresponding to Region A. Only the flow in Region A will be taken into consideration, that is, the geometry will be considered as a pure superposition of six parallel-plate geometries. Torque and rotational speed can be converted to shear stress and shear rate at the rim with the usual equations derived for parallel-plate geometries. It can be shown in Eqs. (1) and (2) that [19]:

$$\text{shear rate at the rim : } \dot{\gamma}_R = \frac{R\Omega}{d} \quad (1)$$

$$\text{shear stress at the rim : } \tau_R = \frac{1}{\alpha} \frac{2C}{\pi R^3} \quad (2)$$

where  $R$  is the radius of the plates,  $\Omega$  is the angular velocity,  $d$  is the shear gap,  $C$  is the torque, and  $\alpha$  is the number of “components” used. The factor  $1/\alpha$  restores the value of the torque measured when several couples of parallel plates are used to the value corresponding to a single one.

The three external axes that support the turning plates may give rise to end effects. It is difficult to estimate the importance of these effects analytically, but one can expect them to be low because the three axes “see” only a small part of the circumference of the plates. Moreover, the contact of the sheared part of the sample with the bulk non-sheared suspension gives rise to edge effects that cannot be estimated analytically. These error-introducing effects will be quantified with the calibration process described below.

In a torsional flow, the shear rate is not constant throughout the sample. Specifically, it varies from 0 at the center of the plates to its maximum value at the rim. Consequently, for a non-Newtonian fluid, corrections have

to be made to account for this gradient. Assuming that cement slurries are power-law fluids (described by Eq. (7)), the following correction, proposed by Weissenberg, can be applied. He suggests that the shear stress given by Eq. (2) should be multiplied by  $0.75 \times n$ . For oil well cement pastes, similar to those used in this work, we find in the literature [1,20]  $n$  values that lie between 0.1 and 0.9. Using these values of  $n$  estimate the viscosity over-estimation from 2% to 22%. However, the errors are smaller in reality [21]. Cement slurries exhibit a significant viscosity reduction with shear rate until a value of shear rate (about  $1 \text{ s}^{-1}$  for our slurries) and a near-Newtonian behavior for high shear rates. Having in mind that in our geometry the central part of the plates, where shear rates are close to zero, is eliminated, the errors should be almost negligible when working at shear rates higher than  $1 \text{ s}^{-1}$ . No correction for the non-Newtonian behavior has been taken into account in this work.

Several repeatability tests have been carried out with Newtonian fluids (glucose solutions). The results were reproducible with a relative error of less than 10%. This value is very close to the systematic error of any commercial rheometer operating with a classic geometry.

For the calibration of the new device, we used Newtonian glucose solutions with viscosity from 0.08 to 1.50 Pa s that is of the same order of magnitude as the cement pastes used [22]. Measurements were carried-out at shear rates from  $10^{-3}$  to  $10^2 \text{ s}^{-1}$ . The results of the new geometry were compared to the results of a cone and plate geometry. Values obtained with the new geometry were systematically elevated in comparison to the cone and plate values. The difference ranges from 8% to 17%, according to the solution. This error may be attributed to the edge effects as well as to the extra torque produced by the shearing of the sample between the internal ribs of the plates and the central axis or the external ribs of the plates, and the three supporting axes. This error is subtracted in the following by systematically multiplying the results with a

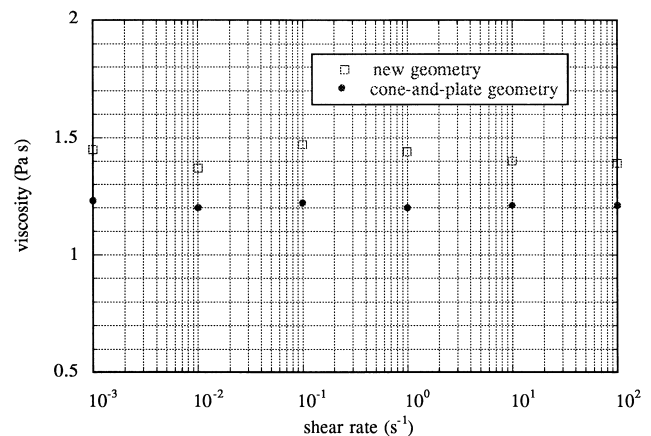


Fig. 3. Comparison of flow curves of a glucose solution obtained with a conventional cone-and-plate geometry and the new geometry.

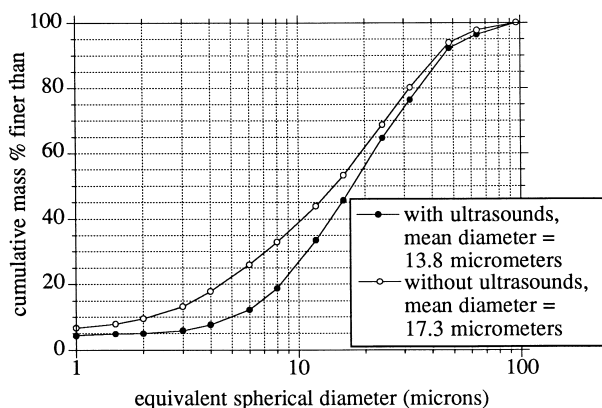


Fig. 4. Particle size distribution of the cement used.

correction factor. This factor is the mean value of the correction factors calculated for each calibration solution, namely 0.9. The results obtained for one of these solutions are shown in Fig. 3.

### 2.3. Evaluation of the new geometry

Tests were performed to evaluate the new geometry.

A Dyckerhoff Class G oil well cement was used for the experiments. The pastes were prepared by mixing deionized water, cement, and two commercial additives according to the American Petroleum Institute (API) [23] requirement 10, Section 5. The water-to-cement ratio was 0.44. The additives used are a set retarder (modified lignosulfonate) and a filtrate reducer (hydroxyethylcellulose). The commercial names of these additives are D800 and D059 (supplied by Dowell Schlumberger), respectively. They were added at 0.55% by weight of dry cement. Physical properties of the cement and slurries are listed in Table 1. Light-scattering particle size distribution of the cement is given in Fig. 4.

A study of the settlement process has been undertaken with the following tests, which were carried out with the Carrimed CS100 rheometer. With these tests, the time during which results are not affected by settlement can be determined. The experimental procedure consists in applying a constant shear stress on the rotating part, and recording the generated shear rate during approximately 90 min. This procedure is repeated using the two upper, two middle, or

Table 1  
Physical properties of cement and slurries used

<i>Dry cement</i>	
Mass median diameter ( $\mu\text{m}$ )	17.3
Density ( $\text{kg/m}^3$ )	3200
Surface area ( $\text{m}^2/\text{kg}$ )	1420
<i>Slurry</i>	
Density ( $\text{kg/m}^3$ )	1920
Volume fraction (%)	41
Concentration (% by weight)	69

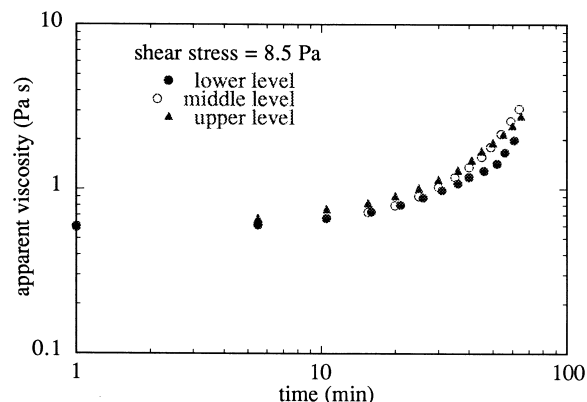


Fig. 5. Constant shear stress experiments performed in three different levels of the sample.

two lower components of the geometry. Thus, measurements take place in the upper, middle, or lower layer of the sample, respectively. Because the settlement process depends on the intensity of the shear, tests were run at various values of shear stress. The results are presented in Figs. 5, 6, and 7. The results are presented in terms of apparent viscosity as a function of time.

When a low shear stress is applied (Fig. 5), the three curves have approximately the same evolution during the experiment. The apparent viscosity increases continuously with time. The same increase is measured in the three levels. This increase is due to the formation of weak electrostatic and/or chemical bonds between cement grains. At low shear stress, thus, a three-dimensional network is allowed to form. This network supplies a stress that balances the gravity force exerted on a coarse particle, and the particle does not settle. On the contrary, at higher shear stresses, the three curves coincide during the first few minutes of the experiments, but they completely deviate afterwards (see Figs. 6 and 7). This deviation is associated with the difference in concentration caused by the settlement of cement particles. In the begin-

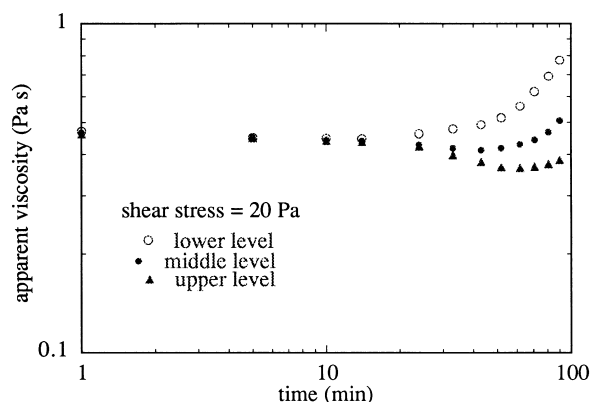


Fig. 6. Constant shear stress experiments performed in three different levels of the sample.

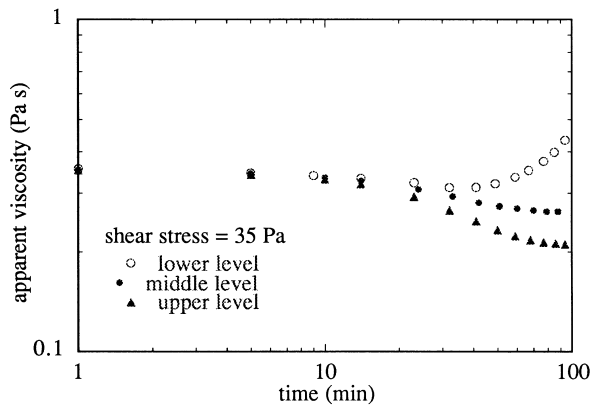


Fig. 7. Constant shear stress experiments performed in three different levels of the sample.

ning of the experiment, the particle concentration is homogeneous. As fast as the shear is applied, particles migrate towards the lower layers. That creates a concentration gradient along the axial direction. The upper layer becomes thinner, and the lower thicker.

Measurements performed throughout the whole sample can be considered meaningful for as long as the three curves coincide. After that time, the heterogeneity of the sample produces erroneous results.

The second type of tests consists in comparing constant rotational velocity curves obtained using the new geometry and a conventional parallel-plate geometry. The Weissenberg rheogoniometer was used for these tests.

With the classical parallel-plate geometry, we have tried to combat slip at the walls and evaporation as described in Ref. [22]. More particularly, the surface of the plates was covered with abrasive paper of a mean grain size of  $200\ \mu\text{m}$  in order to reduce wall slip effects. A protection system against evaporation was also used. That was a transparent plastic cylinder with a cover, which we place around the plates holding the sample. A part of its surface was sponge-coated. The sponge

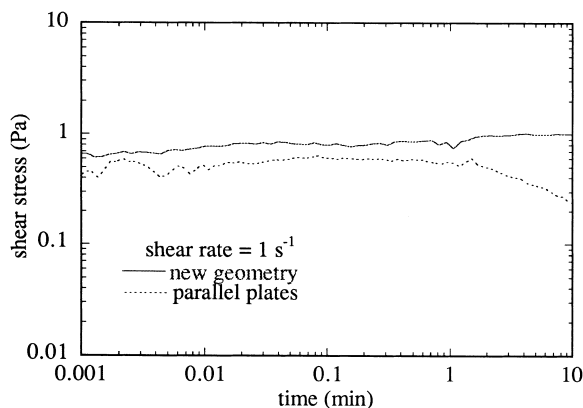


Fig. 8. Comparison of constant shear rate curves obtained with the new geometry and a conventional parallel-plate geometry.

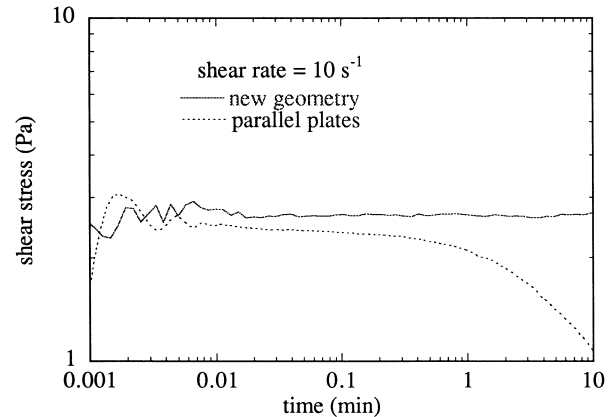


Fig. 9. Comparison of constant shear rate curves obtained with the new geometry and a conventional parallel-plate geometry.

was impregnated with water to saturate the atmosphere around the sample and prevent it from drying out.

With new geometry, the problem of evaporation is minimized by the conception of the fixture. The part of the sample where measurements take place is not in contact with surrounding air. The only free surface is the top surface of the sample holder, which is not involved in the measurement. However, in order to avoid the drying-out of this surface, a thin layer of oil was poured on the top of the cement. Only the two middle “components” of the geometry have been used for the following tests to minimize the influence of the settlement.

Figs. 8 and 9 present the results of these experiments. Shear rates of 1 and  $10\ \text{s}^{-1}$  (shear rates at the rim of the plates) was imposed for 10 min. It has to be made clear that, in reality, we impose the rotational speed that would lead to the desired shear rate, if no slip or other trouble-making effect intervenes.

It is clear that the two geometries lead to diverging results. The difference in the measured viscosity turns out to be very important for tests lasting more than 1 min. This difference can be explained as follows: for the conventional parallel-plate at the beginning of the test, the sample is homogeneous and correctly sheared throughout its volume. After some seconds of shearing, sediment is formed on the surface of the lower plate and a depleted layer appears under the surface of the upper plate. Shear is localized in the thin, depleted layer of supernatant of much lower concentration than the original suspension.

### 3. Conclusions

This work has been undertaken to develop a new rheometric geometry, likely to answer efficiently to the problem of settlement in suspensions of coarse, heavy particles. The basic idea is to use “permeable,” grid tools located in the bulk of samples. More specifically, tools with walls perme-

able from the settling particles, and immersed in a cup containing the sample were used. The particles are free to settle through the plates, but measurements take place away from the upper and lower zones that are affected by this migration. In the measurement zone, the sample can be considered as homogeneous during a period of time that depends on the characteristics of the suspension. In other words, the geometry does not act against settlement but spares measurements from its influence.

Using these principles, a modified parallel-plate geometry was built. This device was used to characterize oil well cement slurries in the present work and in Refs. [11,22]. Tests were performed in parallel with tests on conventional instruments. The results reveal that the conventional geometries can give erroneous and misleading results. The new geometry provides error-free measurements if the duration of the experiment is adapted to the characteristics of the suspension and to the shear conditions.

The new geometry allowed us to study the settling process of the cement slurries as a function of the intensity of the shear.

## Appendix A. Derivation of the equations

The flow in Region B (Fig. 2) is a flow generated between two coaxial rotating cylinders. The shear rate on the surface of the inner cylinder is given by Eq. (3) (the radii  $R_1$ ,  $R_2$ ,  $R_3$ , and the shear gaps,  $d_2$  are indicated in Fig. 2):

$$\dot{\gamma}_{R_1} = \frac{2\Omega}{1 - \beta^2}, \text{ where } \beta = \frac{R_1}{R_2} \quad (3)$$

and the torque on the cylinder of radius  $R_1$  is shown in Eq. (4):

$$C_B = 2\pi R_1^2 d_1 \tau_{R_1} \quad (4)$$

The flow in Region A is a torsional flow. The equations describing it are Eqs. (5) and (6).

$$\text{shear rate at the rim : } \dot{\gamma}_{R_3} = \frac{R_3 \Omega}{d_2} \quad (5)$$

$$\text{torque : } C_A = \int_{R_2}^{R_3} 2\pi r^2 \tau_r dr \quad (6)$$

The complete development of these calculations is presented, for example, in Walters [19] or Piau [24].

We will try to estimate the relative importance of these two parts on the global torque. Let us assume that cement pastes follow a power law of the form:

$$\tau = K \dot{\gamma}^n. \quad (7)$$

In this case, we have Eqs. (8) and (9):

$$C_B = 2K \frac{\pi R_1^2 d_1}{(1 - \beta^2)^n} 2^n \Omega^n \quad (8)$$

$$C_A = \frac{2\pi R_3^3}{3 + n} K \left( \frac{R_3 \Omega}{d_2} \right)^n \text{ because } R_3^3 \gg R_2^3. \quad (9)$$

The ratio of these two quantities can provide an estimation of their relative importance (see Eq. (10)).

$$\rho = \frac{C_B}{C_A} = (n + 3) \left( \frac{d_2 R_2}{(R_2 - R_1) R_3} \right)^n \left( \frac{R_1}{R_2} \right)^2 \frac{d_1}{R_3} \quad (10)$$

(by assuming  $\beta \approx 1$ ).

The numerical values of the symbols are  $d_1 = 1.5$  mm,  $d_2 = 2$  mm,  $R_1 = 4$  mm, and  $R_2 = 7$  mm,  $R_3 = 28$  mm.

For oil well cement pastes, similar to those used in this work,  $n$  values that lie between 0.1 and 0.9 are reported in the literature [1,20].

Substituting the numerical values to the expression of  $\rho$ , we get  $6 \times 10^{-4} < \rho < 2 \times 10^{-3}$ , i.e.,  $\rho \ll 1$ . Therefore,  $C_B$  can be neglected in the calculation of the global torque.

## References

- [1] J.A. Orban, P.A. Parcevaux, Viscometers evaluated for accurate determination of cement slurry rheology, *Oil Gas J* 30 (1986) 94–100 (June).
- [2] G.H. Tattersall, P.F.G. Banfill, *The Rheology of Fresh Concrete*, Pitman Adv. Publ. Prog., London, 1983.
- [3] J.H. Denis, D.J. Guillot, Prediction of cement slurry laminar pressure drops by rotational viscometry, *SPE/IADC* 16137.
- [4] R.J. Mannheimer, Laminar and turbulent flow of cement slurries in large diameter pipe — a comparison with laboratory viscometers, in: P.F.G. Banfill (Ed.), *Rheology of Fresh Cement and Concrete*, E & FN Spon, London, 1991, pp. 147–157.
- [5] P.F.G. Banfill, D.R. Kitching, Use of a controlled stress rheometer to study the yield stress of oil-well cement slurries, in: P.F.G. Banfill (Ed.), *Rheology of Fresh Cement and Concrete*, E & FN Spon, London, 1991, pp. 125–135.
- [6] D. Leighton, A. Acrivos, The shear-induced migration of particles in concentrated suspensions, *J Fluid Mech* 181 (1987) 415–439.
- [7] J.R. Phillips, C.R. Armstrong, A.R. Brown, A constitutive equation for concentrated suspensions that accounts for shear-induced particle migration, *Phys Fluids A* 4 (1991) 30–40.
- [8] D.M. Husbant, L.A. Mondy, E. Ganani, A.L. Graham, Direct measurements of shear-induced particle migration in suspensions of bimodal spheres, *Rheol Acta* 33 (1994) 185–192.
- [9] A. Acrivos, Shear-induced particle diffusion in concentrated suspensions of non-colloidal particles, *J Rheol* 39 (1995) 813–824.
- [10] P. Coussot, J.-M. Piau, A large-scale coaxial cylinder rheometer for the study of the rheology of natural coarse suspensions, *J Rheol* 39 (1995) 105–124.
- [11] P.V. Vlachou, *Rhéologie des Laitiers de Ciment Pétrolier*, PhD Thesis, INPG, France, 1996.
- [12] J.I. Bhatti, P.F.G. Banfill, Sedimentation behavior in cement pastes subjected to continuous shear in rotational viscometer, *Cem Concr Res* 12 (1982) 69–78.
- [13] G.H. Meeten, Rheometer, Br. Patent Application No. UK 9026294.0, 1990.
- [14] J.-M. Piau, Crucial elements of yield stress fluid rheology, in: M.J. Adams, R.A. Mashelkar, J.R.A. Pearson, A.R. Rennie (Eds.), *Dynamics of Complex Fluids*, Imperial College Press — The Royal Society, London, 1997, pp. 351–371.
- [15] S. Ducerf, J.-M. Piau, *Les Cah Rheol*, XIII 1–2 (1994) 120–129.

- [16] S. Ducerf, Etude des Propriétés Rhéométriques de Suspensions Aqueuses Minérales Microniques Denses, en Fonction de leurs Propriétés Structurales, PhD Thesis, INPG, France, 1996.
- [17] B. Klein, J.S. Laskowski, S.J. Partridge, A new viscometer for rheological measurements on settling suspensions, *J Rheol* 39 (1995) 827–840.
- [18] J.C. Maxwell, On the viscosity or internal friction of air and other gases, *Philos Trans R Soc London* 156 (1866) 1–25.
- [19] K. Walters, *Rheometry*, Chapman & Hall, London, 1975.
- [20] A.M. Haimoni, Rheology of a specific oil-well cement, PhD Thesis, Department of Civil Engineering, University of Surrey, 1987.
- [21] P. Coussot, J.-M. Piau, Techniques de rhéométrie en cisaillement simple dans le cas de dispersions et suspensions concentrées, *Les Cah Rheol*, XII 1 (1993) 1–13.
- [22] P.V. Vlachou, J.-M. Piau, The influence of the shear field on the microstructural and chemical evolution of an oil well cement slurry and its rheometric impact, *Cem Concr Res* 27 (1997) 869–881.
- [23] American Petroleum Institute (API), Specification for Materials and Testing of Well Cements, API Spec. 10, 3rd edn., American Petroleum Institute, Washington, DC, 1987 (August).
- [24] J.-M. Piau, Fluides non-Newtoniens, *Tech Ing, A* (1979) 710–711.